HYDRAULIC PERFORMANCE DETERIORATION OF CERAMIC FILTERS: EXPERIMENTAL INSIGHTS AND FOULING MODEL DEVELOPMENT

Rahul Chakrabarty*[1], Quazi Hamidul Bari[2], and Md. Al Amin[3]

[1] *Postgraduate Student, Department of Civil Engineering, Khulna University of Engineering & Technology (KUET), Khulna, Bangladesh, e-mail: ck.rahul18@gmail.com*
[2] *Professor, Department of Civil Engineering, Khulna University of Engineering & Technology (KUET), Khulna, Bangladesh, e-mail: qhbari@ce.kuet.ac.bd*
[3] *Postgraduate Student, Department of Civil Engineering, Khulna University of Engineering & Technology (KUET), Khulna, Bangladesh, e-mail: mdalamin2308@gmail.com*

***Corresponding Author**

ABSTRACT

In many underdeveloped nations where households depend on untreated surface water with high turbidity, access to clean drinking water is still a chronic problem. Although simple ceramic filters (CFs) provide a cost-effective point-of-use (POU) option, turbidity-induced blockage greatly affects their hydraulic performance. This work creates a predictive fouling model to explain flow-rate reduction and investigates how rising turbidity impacts a clay-rice-bran ceramic filter's flow performance. 80% clay and 20% rice bran were combined to make the ceramic filter, which was then burned to provide a porous filtration structure. Experiments were carried out in the lab with constant head circumstances in water with turbidity levels ranging from low to severely murky. The starting flow rate of 1.3712 L/h for clean water decreased exponentially as turbidity rose. The flow rate decreased by 35% to around 0.90 L/h at 100 NTU. Based on the exponential relation $Q = Q_0\, e^{-\beta T}$, the fouling sensitivity coefficient (β) averaged 0.004 (1/NTU) with a significant correlation ($R^2 > 0.99$), indicating that turbidity is the main cause of short-term clogging. To replicate real-world filtering behavior, a mechanistic model was created that combined Darcy flow with turbidity-dependent fouling (βT) and time-driven clogging (γt). Both the initial quick fall in flow rate and the slower long-term decay were accurately captured by model predictions, which closely matched experimental findings. Strong agreement between projected and measured values was indicated by the statistical evaluation's good predictive performance (RMSE = 0.0812 L/h; MAPE = 5.87%; R^2 = 0.9933). The study clearly demonstrates that even during brief operating periods, turbidity dramatically impairs the hydraulic performance of ceramic filters. The suggested model helps the development of inexpensive ceramic filtration technologies in turbidity-prone conditions and offers a trustworthy tool for forecasting flow decline. These results can direct design enhancements and guarantee more reliable and sustainable production of drinking water for homes.

Keywords: *Ceramic filter, Turbidity, Flow rate, Fouling model, Point-of-use water treatment*

1. INTRODUCTION

Individual health depends on having access to clean drinking water. The quality and quantity of safe drinking water sources are among the biggest issues the world is now experiencing (Chakrabarty & Mohiuddin, 2024). In developing nations, the regular contamination of surface water sources, such as ponds and lakes, poses a significant public health concern. For instance, just 53% of people in rural regions have access to clean drinking water, compared to 85% of those in metropolitan areas worldwide (Yang et al., 2020). Generally, pond water is used for bathing and toothbrushing, and is often not utilized for cooking or drinking. In southern Bangladesh, some families use pond water as an additional source of water for cooking and drinking. Consumers of drinking water from various insecure sources may be exposed to potentially dangerous inorganic and organic pollutants, which can originate from human activities (anthropogenic) or natural processes (geogenic) (Gwenzi et al., 2021). Waste from residential and commercial sources pollutes surface water, but wastewater pretreatment can reduce this impact (Chakrabarty & Bari, 2025). They may also be at risk from pathogenic organisms, toxic metals, or other life-threatening contaminants. The World Health Organization states that contaminated water can transmit over 80 fatal diseases (WHO, 2018).

Field trials of both higher- and lower-cost filters indicate that low-cost, locally produced filters can improve household access to safe water, offering advantages in cost, local materials, and community entrepreneurship. Around the world, several methods of treating domestic water are employed, including boiling, chlorination, and bio-sand filtration. Household or point-of-use (POU) water treatment technologies treat and protect stored water from microbial and chemical contamination, even when source water is safe (Wright et al., 2004). They are crucial where piped systems are unavailable or unsafe, offering significant potential health benefits in developing countries (Sobsey, 2006). POU water treatment technologies, such as the Ceramic Water Filter (CWF), are therefore viable ways to provide rural, impoverished people with clean drinking water (Amin et al., 2023; Chakrabarty & Bari, 2025; Farrow et al., 2014; Berg, 2015). It's gained wide acceptance due to its simple design, low cost, and local manufacturability. Usually, combustible organic materials like rice husk, sawdust, rice bran, or paper fibers are mixed with locally accessible clay to create ceramic filters (Oyanedel-Craver & Smith, 2008). Then, during firing at high temperatures (about 800-900°C), it burns off, generating the thin porous structure essential for effective filtering (Yang et al., 2020). Particulate matter and bacteria can be effectively removed by the pore structure, and arsenic adsorption and co-precipitation are enabled by the inclusion of iron-based components. A significant advancement in this area is the iron-modified ceramic filter, which combines a ceramic candle with an iron mesh or iron bacterial sludge. Biofilm growth on the CWF surface enhances pathogen removal, with silver nitrate or nanoparticles sometimes added for additional disinfection (Oyanedel-Craver & Smith, 2008; Rayner et al., 2013).

Surface water now has higher levels of turbidity, toxicity, and trace metals due to untreated urban waste, industrial effluents, and agricultural runoff (Islam et al., 2015). One of the most common issues with these water filtration methods is elevated turbidity, which is directly connected to and caused by suspended organic debris, total suspended solids, electrical conductivity, clay, silt, and colloidal particles. High turbidity not only reduces aesthetic appeal but also renders residential water treatment systems less useful and efficient. Households may find it more challenging to obtain adequate drinking water each day due to increased particle loading, which can clog filter media, reduce hydraulic conductivity, and significantly lower flow rates (WHO, 2018). The relationship between turbidity and flow rate is particularly significant since flow rate directly affects household acceptance, daily water supply capacity, and system adherence. According to Brown and Sobsey (2009), the flow rate dramatically dropped as influent turbidity increased over 50 NTU. When a filter becomes too slow due to obstruction, many quit using it, even if the treatment efficacy is still very good. Additionally, a decreased flow rate may increase the likelihood of microbial formation on the filter surface due to prolonged water stagnation (Bielefeldt et al., 2009). The majority of research has focused on the microbiological removal capacities of ceramic filters; very few have examined hydraulic behavior and clogging dynamics under various turbidity conditions. Therefore, knowing how turbidity and filter performance are related is essential to developing affordable water treatment solutions.

The primary goal of this research is to assess the detrimental impacts of raising raw-water turbidity on the flow rate and the performance of simple ceramic filters, which are frequently utilized for drinking

water purposes in households. Compared with the field study and laboratory tests, findings show a decremental relationship in flow rate with increasing turbidity. Understanding this relationship is crucial for improving any further filter technology modifications, especially by balancing the design trade-off. By carefully quantifying the drop in flow efficiency throughout a range of turbidity conditions, the study aims to give vital information for predicting filter behavior linked to pore clogging and permeability loss. In the end, this will help meet public health concerns by ensuring a more consistent and reliable supply of simple ceramic-filtered drinking water.

2. METHODOLOGY

2.1 Simple Ceramic Filter

Point-of-use (POU) of ceramic water filters (CWFs), which may be produced by local clay mixed with fine organic materials like sawdust or rice husk, has gained widespread popularity over the past 20 years as an inexpensive method to clean microbially tainted water (Bielefeldt et al., 2009; Oyanedel-Craver & Smith, 2008; Amin et al., 2023). All of these components mix, and when the ceramic is fired, the organics burn off and leave behind small, interconnected pores. This ceramic filter was made by mixing 80% clay soil and 20% rice bran, sourced from a local brick field and a nearby rice mill in southern Khulna, Bangladesh (Shafiquzzaman et al., 2011). Soil and rice bran were completely combined until homogeneous in order to fulfill the purposes. The resultant cylindrical filters were 10 cm tall and 2 cm thick, hollow, and had one open end (Figure 1. b) (Shafiquzzaman et al., 2011). The ceramic filter's apparent porosity was assessed in accordance with Yang et al. (2007), and the pore size of the filter was calculated by comparing the particle size distribution of turbid water (including clay) before and after filtering.

2.2 Filter Setup Process

The first stage of the manufactured ceramic filter is fastened to the plastic bucket's bottom (Figure 1. a, b). The open end of the CF is joined to the inner bottom plastic surface using glue gum. The CF unit was placed atop a steel platform with the closed end in the top position. To collect the effluent, an extra plastic bucket was positioned just below the platform. Initially, fill the ceramic-attached bucket with zero ionized or distilled water, then gauge the flow rate in milliliters per minute. It is carried out three times at the same water level in the bucket to guarantee accuracy. The flow rate is then measured using the turbid water. For every set turbidity value, three trials were carried out, and the average was used to figure out the flow rate at this turbidity.

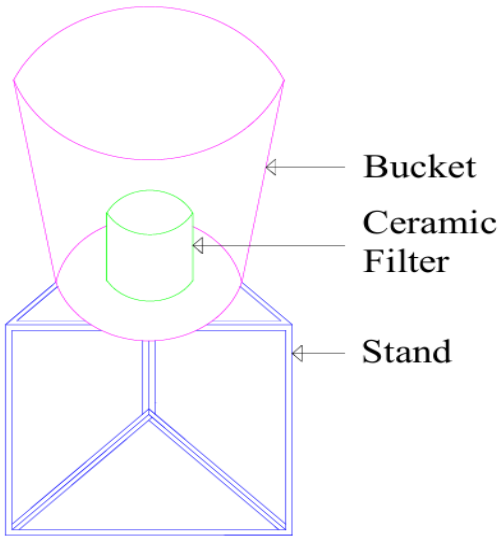

Figure 1 (a): Ceramic Filter in Plastic Bucket.

Figure 1 (b): Ceramic Filter in Plastic Bucket.

2.3 Fouling Dynamics Model

For this analysis, this study employed a simplified phenomenological model of fouling to fully explore the role of influent turbidity in hydraulic performance using the simple ceramic filter. Initially, the volumetric flow rate (Q_0) was first determined using distilled water passing through the porous wall of the ceramic filter at a constant hydraulic head in the laboratory. When filtering turbid water, suspended particles and other colloidal debris gradually accumulate on or within the pores of a simple ceramic filter. This process forms a fouling layer that escalates the hydraulic resistance of the medium, consequently reducing the measured flow rate to a new value, Q (L/h).

From previous research and literature review, an assumption has been made that the current flow rate is directly proportional to the incremental decrease in flow rate resulting from a small increase in turbidity. This suggests that the addition of each new unit of turbidity (i.e., more particle load) has a correspondingly equivalent relative influence on the remaining open pore volume as the pores get smaller. Mathematically, this assumption can be expressed as Equation 1.

$$\frac{dQ}{dT} = -\beta Q \tag{1}$$

Where T is the influent turbidity (NTU), and β is a fouling-sensitivity coefficient (1/NTU) that characterizes the extent to which turbidity affects the flow rate.

Rearranging Eq. (1) gives-

$$\frac{1}{Q} dQ = -\beta \, dT \tag{2}$$

Integrating Eq. (2) when $Q = Q_0$ at $T = 0$ (clean / distilled water) and $Q = Q$ at turbidity T yields.

$$\int_{Q_0}^{Q} \frac{1}{Q} dQ = -\beta \int_{0}^{T} dT$$

$$\ln \frac{Q}{Q_0} = -\beta T \tag{3}$$

Exponentiating both sides leads to the ***Exponential Decay Relationship*** between flow rate and turbidity.

$$Q = Q_0 \, e^{-\beta T} \tag{4}$$

In this study, the decrease in flow rate as a function of influent turbidity is predicted using Equation 4. Constant-head filtration experiments using deionized or extremely low-turbidity water yield the parameter Q_0, whereas nonlinear regression (or linear regression of $\ln(Q/Q_0)$ versus T) using experimental pairings of (T, Q) yields β.

Over time, the buildup of suspended solids (SS) and other colloidal debris on the ceramic filter surface raises the hydraulic resistance in addition to turbidity-related fouling. This time-dependent clogging effect is incorporated into the extended model as

$$Q = Q_0 \, e^{(-\beta T + \gamma t)} \tag{5}$$

where γ is the time-dependent fouling coefficient due solely to suspended solids deposition on the filter surface, and t is the filtration time (days).

The final model equation combines the effects of turbidity-induced and time-dependent fouling with ***Darcy-based*** mechanical flow to predict the flow rate through the ceramic filter. The flow loss due to turbidity (βT) and progressive surface fouling (γt) is represented by the exponential penalty term, whilst the intrinsic permeability of the ceramic filter (k), filter area (A), hydraulic pressure (ΔP), viscosity (μ), and wall thickness (L) are taken into account by the mechanistic term. The complete model is given by Equation 6.

$$Q\,(T, t, A, L) = \frac{kA\Delta P}{\mu L} \, e^{(-\beta T + \gamma t)} \tag{6}$$

In this formulation, A is the active filter surface area (m²), Q is the flow rate (m³/s or L/h), L is the thickness of the ceramic wall (m), k is the intrinsic permeability (m²), $\Delta P = \rho g h$ is the pressure produced by the water head h, and μ is the water's dynamic viscosity (Pa·s). Turbidity sensitivity and time-driven fouling, including biofilm formation and pore blockage, are measured using the parameters β (1/NTU) and γ (1/time). This model demonstrates how the flow rate falls with increasing wall thickness ($Q \propto 1/L$) and rises with a larger filter surface area ($Q \propto A$).

2.4 Model Performance Analysis

The effectiveness of the proposed numerical flow-rate model was evaluated in this study by comparing the projected flow rate values with actual experimentally collected data. Several widely used statistical metrics, including mean square error (MSE), root mean square error (RMSE), mean absolute deviation (MAD), and mean absolute percentage error (MAPE), were employed to assess the predictive capability of the model objectively as Equations (7-10). MAD was used to represent typical error, RMSE to assess the presence of large or catastrophic errors, and MAPE to express model accuracy in an intuitive percentage form for non-technical interpretation. When applied to the filtered data, these metrics provide a comprehensive evaluation of the model's accuracy, robustness, and error characteristics. The size of the average squared and root-mean-squared disparities between the actual flow rate (Q_i) and the projected flow rate ($\hat{Q}_i$) is shown by the MSE and RMSE. A better fit between the model outputs and the observed data is shown by lower MSE and RMSE values. The average absolute deviation, or MAD, is a helpful tool for comprehending the overall size of prediction mistakes without highlighting greater variances. In the meantime, MAPE allows for a normalized comparison of datasets and filtering settings by expressing the mistake as a percentage of the actual value. A lower MAPE number indicates a more accurate prediction performance. To further assess the strength of the relationship between anticipated and observed flow rates, the coefficient of determination (R^2) was also calculated. An R^2 value of 1 indicates strong agreement between the model predictions and the data collected from experiments, whereas values near 0 indicate poor correlation. A higher R^2 in this study denotes how effectively the numerical model reproduces the flow-decay pattern caused by turbidity and time-dependent obstruction. The statistical indices used in this study were calculated using the following standard formulations:

$$\text{MSE} = \frac{1}{n}\sum_{i=1}^{n}(Q_i - \hat{Q}_i)^2 \tag{7}$$

$$\text{RMSE} = \sqrt{\frac{1}{n}\sum_{i=1}^{n}(Q_i - \hat{Q}_i)^2} \tag{8}$$

$$\text{MAD} = \frac{1}{n}\sum_{i=1}^{n}\left|Q_i - \hat{Q}_i\right| \tag{9}$$

$$\text{MAPE} = \frac{1}{n}\sum_{i=1}^{n}\left|\frac{Q_i - \hat{Q}_i}{Q_i}\right| \tag{10}$$

Here, Q_i denotes the measured flow rate, $\hat{Q}_i$ represents the predicted flow rate from the numerical model, and n is the total number of experimental observations. All things considered, the investigation of these statistical characteristics permits an in-depth evaluation of the numerical model and provides insight into its applicability for forecasting ceramic filter performance under various turbidity and clogging circumstances.

3. RESULTS

3.1 Fouling Sensitivity Coefficient

Figure 2(a) illustrates the relationship between influent turbidity and the associated flow rate of a new ceramic filter. In zero turbidity, the flow rate was found to be Q_0 = 1.3712 L/h. The results clearly show that as turbidity increases, the hydraulic performance of the ceramic filter decreases monotonically. With low turbidity (≈0-10 NTU), the initial flow rate remains fairly high (≈1.35-1.32 L/h). But as turbidity gradually rises to 100 NTU, the flow rate drops to about 0.90 L/h. The strong linear fit (R^2 = *0.9985*) confirms that suspended solids (SS) consistently accumulate on the filter wall, increasing hydraulic resistance even during short-term operation. This pattern demonstrates that turbidity is the primary factor affecting instantaneous flow rate, even when a fresh filter is used for each test. Figure 2(b) illustrates the fouling sensitivity coefficient (β) as a function of turbidity. The coefficient was calculated for each turbidity state based on the proportional drop in flow rate. A clear upward trend indicates that higher turbidity increases the short-term fouling potential. The average β value of ≈0.004 (1/NTU) indicates a mild but detectable fouling response, while the regression line (R^2 = 0.9946) demonstrates a significant relationship between influent turbidity and fouling sensitivity. This high goodness-of-fit suggests that β could be a reliable predictive indicator of turbidity-induced clogging in ceramic filtering systems. The results collectively demonstrate that even new ceramic filters immediately lose efficiency as turbidity increases, and the fouling sensitivity coefficient provides a useful indicator for incorporating turbidity-dependent clogging to mechanistic and predictive filtering models.

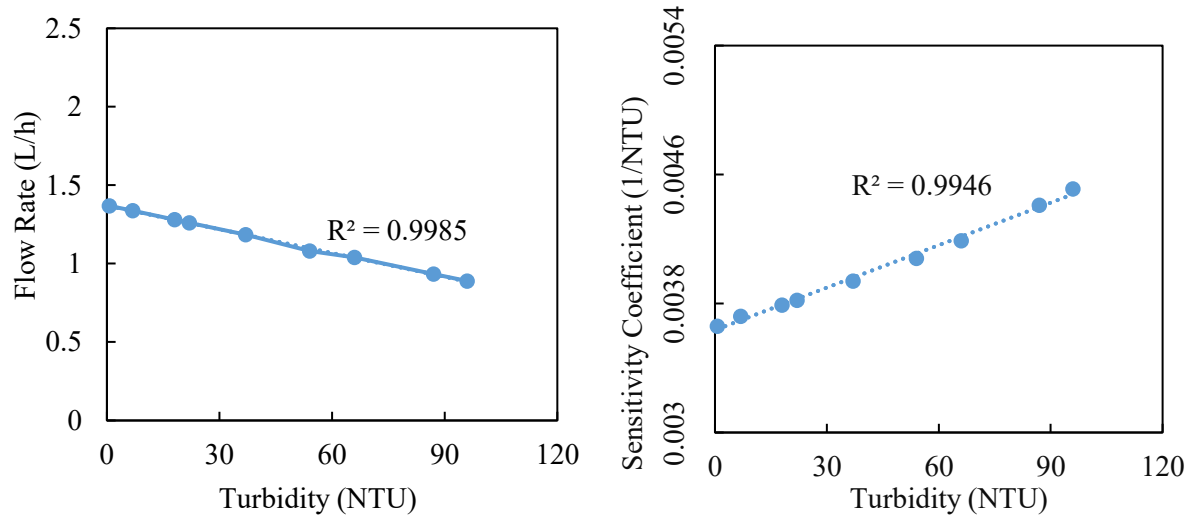

Figure 2: a) Flow rate effect with Turbidity; b) Fouling Sensitivity Coefficient for Turbidity

3.2 Model Output

The model developed in the current study correctly predicts the reduction of output flow rate due to the influence of both the turbidity level and the filtration time. The mechanistic model of fouling honors the hydraulic characteristics of the ceramic filters because there is high agreement between the model-predicted flow rates and the corresponding actual behavior in the experiments. The simulated fluctuation of flow rate about influent turbidity is illustrated in the first model output (Figure 3.a). The expected flow rate falls monotonically from around 2.4 L/h to less than 1.0 L/h as turbidity rises from about 1 NTU to 5.5 NTU. The exponential fouling term ($e^{-\beta T}$), which describes the gradual pore constriction brought on by suspended solids, is consistent with this behavior. Turbidity has a significant and rapid impact on hydraulic resistance, as seen by the model line's smooth curve, which replicates the anticipated nonlinear degradation. The second model output (Figure 3.b) illustrates the predicted temporal evolution of flow rate during continuous filtration. Over a 22-day filtration period, the flow

rate steadily declines from an initial value of approximately 2.4 L/h to around 0.9 L/h. This decrease is influenced by a time-dependent fouling component ($e^{-\gamma T}$), which signifies the accumulation of surface deposits and biofilm growth on the inner ceramic structure. The model effectively captures the distinctive early-stage reduction associated with rapid initial clogging, followed by a more gradual decline as the system approaches a stable fouled condition.

Overall, both model outputs show that the numerical formulation effectively captures the combined effects of turbidity loading and long-term fouling on filter performance. The close alignment between predicted and observed flow behavior highlights the model's ability to serve as a reliable tool for predicting the decline in flow rate of ceramic filters under different water quality and operational conditions.

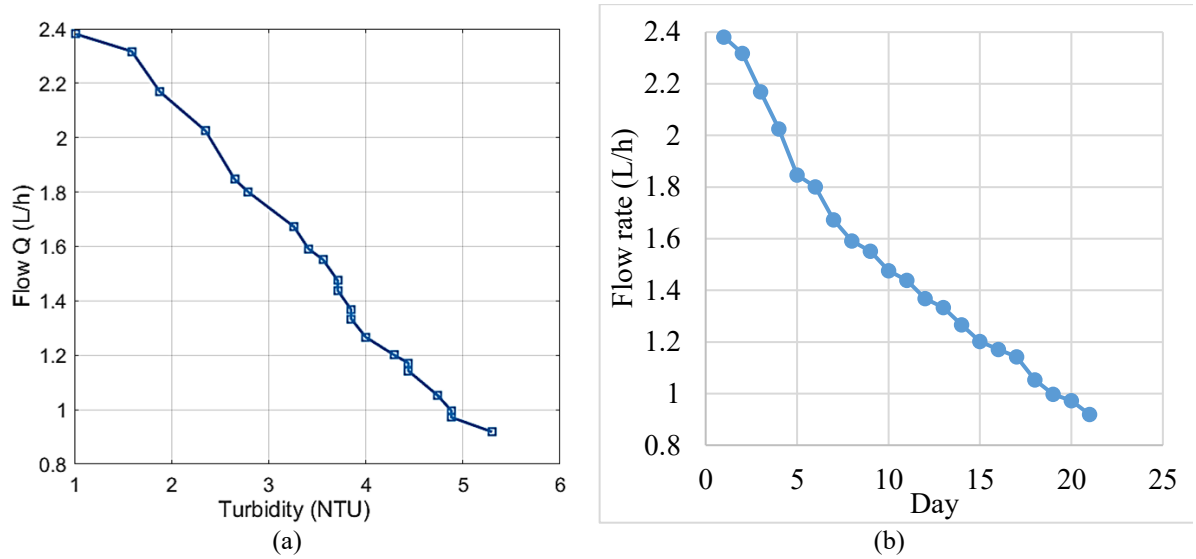

(a) (b)

Figure 3: a) Flow rate variation with respect to Turbidity; b) Flow rate variation per day

3.3 Model Performance

The developed numerical model's prediction power was evaluated by contrasting the calculated flow-rate values with the data obtained through experimentation. The findings show that the flow-rate reduction that occurs during ceramic filtration under different turbidity and operating times may be faithfully replicated by the model. The statistical indicators (*MSE = 0.00660, RMSE = 0.0812 L/h, MAD = 0.0739 L/h, and MAPE = 5.87%*) confirm a consistently low prediction error across all data points (Table 1). The very small RMSE and MAD values indicate that the average difference between the predicted and actual flow rates is minimal, while the MAPE below 10% reflects high reliability in real-time prediction of filtration performance. This steady performance with no notable outliers or severe prediction failures is indicated by the proximity of the MAD and RMSE values. All things considered, these measures verify that the model is extremely dependable and theoretically tuned for real-world flow-rate applications. The coefficient of determination ($R^2 = 0.9933$) further validates the strength of the model, showing that 99.33% of the variability in measured flow rate is captured by the numerical prediction (Figure 4. a). The data points in the scatter plot of actual versus anticipated flow rates closely align with the 1:1 fitted line, indicating an excellent agreement between expected and observed values. This linear trend demonstrates that the model effectively captures the combined effects of time-induced surface fouling and turbidity-dependent resistance. Further insights into the model's temporal accuracy are provided by the day-wise comparison shown in the bar chart (Figure 4.b). Throughout the 21-day filtering period, both the actual and anticipated flow rates exhibit a similar declining trend. The model accurately represents a sharp decrease in flow rates during the initial days, followed by a gradual decline as congestion worsens. Although slight deviations are visible at certain time steps, the overall alignment between the two datasets confirms that the model effectively describes the long-term fouling behaviour of the ceramic filter.

Overall, the statistical metrics, scatter correlation, and day-wise bar comparison all indicate that the proposed mechanistic-fouling model provides a robust, accurate, and reliable tool for predicting flow-rate decay in ceramic water filters under turbidity loading and prolonged operation.

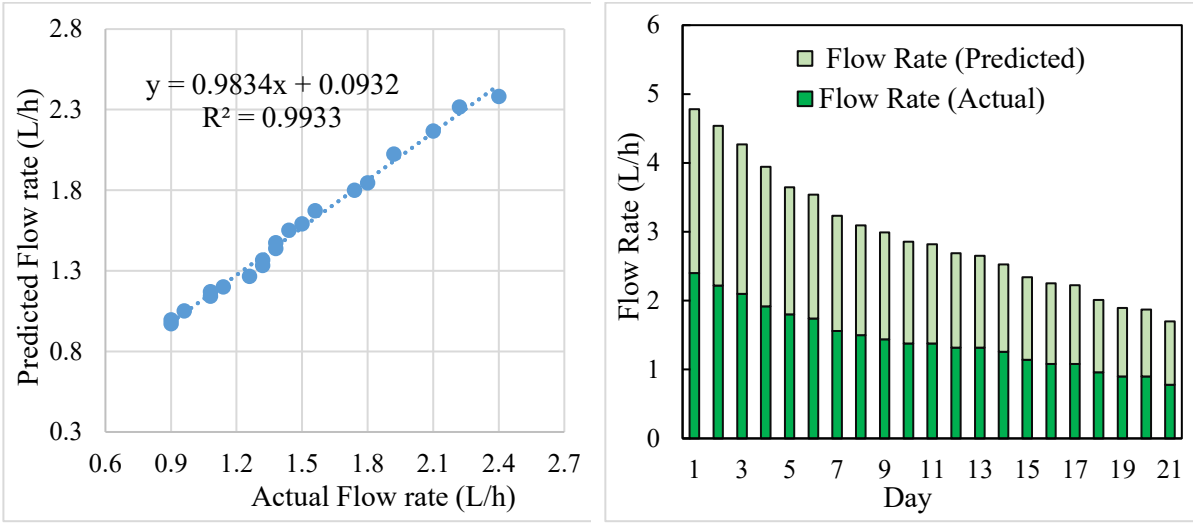

(a) (b)

Figure 4: a) Validity measure by numerical prediction; b) Day-wise comparison of flow rate.

Table 01: Statistical indicators used in the model.

Statistical Indicator	Computed Value
MSE	0.00660
RMSE	0.0812
MAD	0.0739
MAPE	5.87%
R^2	0.9933

4. ENGINEERING SIGNIFICANT

This study introduces a quantified Fouling Sensitivity Coefficient for Turbidity ($\beta \approx 0.004$) for ceramic filters, representing a significant advancement in the predictive modeling of fouling behavior in porous filtration systems (Figure 5). By using this coefficient within a fouling dynamics framework, the model enables robust and computationally efficient prediction of flow-rate degradation under varying turbidity conditions, reducing reliance on extensive experimental calibration. The proposed approach provides a scalable and transferable design tool for evaluating filter performance and guiding data-driven optimization of ceramic filter geometry and operating conditions. Incorporation of fouling sensitivity at the design stage allows engineers to proactively mitigate fouling effects, enhance hydraulic efficiency, and extend operational lifespan, thereby lowering maintenance and lifecycle costs. Beyond ceramic filtration, the methodology establishes a generalizable pathway for deriving fouling sensitivity coefficients for alternative filter materials, supporting cross-material performance comparison and adaptive filter design. The application of these fouling dynamics models enables systematic redesign of filtration systems aligned with sustainability objectives, including improved resource efficiency, reduced material waste, and enhanced long-term system resilience. Collectively, this work contributes a predictive, material-agnostic framework that advances the engineering design and sustainable deployment of filtration technologies.

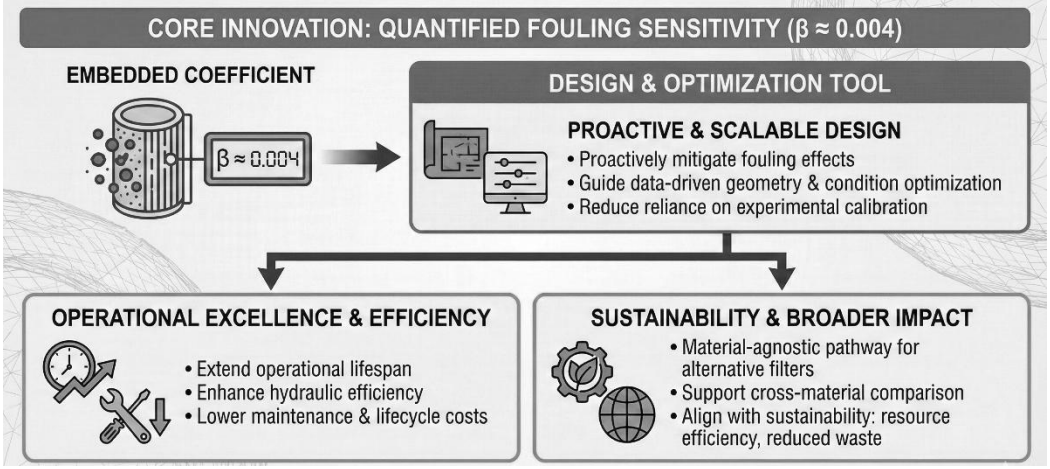

Figure 5: Engineering Significance: Predictive Fouling Dynamics Framework

5. CONCLUSIONS

This study shows that the hydraulic performance of ceramic filters is significantly and immediately impacted by turbidity. The flow rate consistently decreased as turbidity rose, according to experimental data, and the increasing clogging potential under greater suspended-solid and colloidal loads was corroborated by the rising fouling sensitivity coefficient (β). These results demonstrate that turbidity is a major factor in determining short-term filter resistance. Both the long-term fouling behavior and the turbidity-driven flow-rate drop were well replicated by the numerical model. The progressive drop-in flow rate during prolonged operation and the nonlinear decline brought on by particle deposition were both reproduced by simulations. Strong statistical performance (RMSE = 0.0812 L/h, MAPE = 5.87%, R^2 = 0.9933) and close alignment between predicted and observed data support the model's accuracy. Overall, this work supports better filter design and performance management by confirming that turbidity regulates ceramic filter clogging, and the suggested mechanistic model offers a trustworthy tool for forecasting flow-rate reduction.

DECLARATION OF USE OF AI

During the preparation of this work, the authors used some AI tools, such as Grammarly, Quill Bot, Mendeley Cite, etc., for summarization, grammar refinement, spelling correction, and rearranging sentences to improve flow, clarity, and citation management. After using these tools, the authors reviewed and edited the content as needed and take full responsibility for this published article.

REFERENCES

Amin, M. A., Ferdous, J., & Rahman, M. M. Performance Evaluation of a Simple Ceramic Filter (SCF) Combined with Roughing Filter for Pond Water Treatment. Proceedings of the International Conference on Planning, Architecture and Civil Engineering (ICPACE 2023), Rajshahi University of Engineering & Technology, Rajshahi, Bangladesh

Berg, P. A. (2015). The world's need for household water treatment. *Journal-American Water Works Association, 107*(10), 36–44. https://doi.org/10.5942/jawwa.2015.107.0144

Bielefeldt, A. R., Kowalski, K., & Summers, R. S. (2009). Bacterial treatment effectiveness of point-of-use ceramic water filters. *Water Research, 43*(14), 3559–3565. https://doi.org/10.1016/j.watres.2009.04.047

Brown, J., & Sobsey, M. D. (2009). Ceramic media amended with metal oxide for the capture of viruses in drinking water. *Environmental Technology, 30*(4), 379–391. https://doi.org/10.1080/09593330902753461

Chakrabarty, R., & Bari, Q. H. (2025). A review on evaluating cost-effective materials, fabrication, and surface modification for ceramic membrane technology. *Proceedings of International Conference on Civil Engineering Research & Innovations (ICCEI 2025),* Rajshahi University of Engineering & Technology (RUET), Rajshahi, Bangladesh.

Chakrabarty, R., & Mohiuddin, K. ABM. (2024). Techno-economic analysis of a small-scale rainwater harvesting system for producing drinking water at KUET campus. *Proceedings of 7th International Conference on Civil Engineering for Sustainable Development (ICCESD 2024),* Khulna University of Engineering & Technology (KUET), Khulna, Bangladesh.

Farrow, C., McBean, E., & Salsali, H. (2014). Virus removal efficiency of ceramic water filters: Effects of bentonite turbidity. *Water Science and Technology: Water Supply, 14*(2), 304–311. https://doi.org/10.2166/ws.2013.206

Gwenzi, W., Chaukura, N., Wenga, T., & Mtisi, M. (2021). Biochars as media for air pollution control systems: Contaminant removal, applications and future research directions. *Science of the Total Environment, 753*, 142249. https://doi.org/10.1016/j.scitotenv.2020.142249

Islam, M. S., Ahmed, M. K., Raknuzzaman, M., Habibullah-Al-Mamun, M., & Islam, M. K. (2015). Heavy metal pollution in surface water and sediment: A preliminary assessment of an urban river in a developing country. *Eco. Indi., 48*, 282–291. https://doi.org/10.1016/j.ecolind.2014.08.016

Knappett, P. S. K., McKay, L. D., Layton, A., Williams, D. E., Alam, J., Huq, R., Mey, J., Feighery, J. E., Culligan, P. J., Mailloux, B. J., Escamilla, V., Emch, M., & Ahmed, M. (2011). Impact of population and latrines on fecal contamination of ponds in rural Bangladesh. *Science of the Total Environment, 409*(17), 3174–3182. https://doi.org/10.1016/j.scitotenv.2011.04.043

Oyanedel-Craver, V. A., & Smith, J. A. (2008). Sustainable colloidal-silver-impregnated ceramic filter for point-of-use water treatment. *Environmental Science & Technology, 42*(3), 927–933. https://doi.org/10.1021/es071268u

Rayner, J., Zhang, H., Schubert, J., Lennon, P., Lantagne, D., & Oyanedel-Craver, V. (2013). Laboratory investigation into the effect of silver application on the bacterial removal efficacy of filter material for use on locally produced ceramic water filters for household drinking water treatment. *ACS Sustainable Chemistry & Engineering, 1*(7), 737–745. https://doi.org/10.1021/sc400068p

Shafiquzzaman, M., Hasan, M. M., Nakajima, J., & Mishima, I. (2011). Development of a simple, effective ceramic filter for arsenic removal. *Journal of Water and Environment Technology, 9*(3), 333–347. https://doi.org/10.2965/jwet.2011.333

Sobsey, M. D. (2006). Drinking water and health research: A look to the future in the United States and globally. *J. of Water and Health, 4*(Suppl. 1), 17–21. https://pubmed.ncbi.nlm.nih.gov/16493895/

World Health Organization, WHO. (2018). *Developing drinking-water quality regulations and standards: General guidance with a special focus on countries with limited resources.*

Wright, J., Gundry, S., & Conroy, R. (2004). Household drinking water in developing countries: A systematic review of microbiological contamination between source and point-of-use. *Tropical Medicine & International Health, 9*(1), 106–117. https://doi.org/10.1111/j.1365-3156.2004.0126.x

Yang, H., Xu, S., Chitwood, D. E., & Wang, Y. (2020). Ceramic water filter for point-of-use water treatment in developing countries: Principles, challenges and opportunities. *Frontiers of Environmental Science & Engineering, 14*(5), 79. https://doi.org/10.1007/s11783-020-1254-9

Yang, L., Ning, X., Chen, K., & Zhou, H. (2007). Preparation and properties of hydroxyapatite filters for microbial filtration. *Cer. Int., 33*(3), 483–489. https://doi.org/10.1016/j.ceramint.2005.10.014